Aboveground net primary productivity of vegetation along a climate-related gradient in a Eurasian temperate grassland: spatio-temporal patterns and their relationships with climate factors

Tian Gao[1,2,3], Bin Xu[2]*, Xiuchun Yang[2], Songqiu Deng[4], Yuechen Liu[5], Yunxiang Jin[6], Hailong Ma[2], Jinya Li[7], Haida Yu[2], Xiao Zheng[1] & Qiangyi Yu[2]

[1] *Key Laboratory of Forest Ecology and Management, Institute of Applied Ecology, Chinese Academy of Sciences, Shenyang, China;*

[2] *Key Laboratory of Agri-informatics, Ministry of Agriculture / Institute of Agricultural Resources and Regional Planning, Chinese Academy of Agricultural Sciences, Beijing, China;*

[3] *Qingyuan Forest CERN, Chinese Academy of Sciences, Shenyang, China*

[4] *Institute of Mountain Science, Shinshu University, Nagano, Japan;*

[5] *Chinese Academy of Agricultural Engineering, Beijing, China;*

[6] *Agricultural Information Institute, Chinese Academy of Agricultural Sciences, Beijing, China;*

[7] *State Key Laboratory of Urban & Regional Ecology, Research Center for Eco-Environmental Sciences, Chinese Academy of Sciences, Beijing, China*

* Correspondence author at: 12 Zhongguancun South Street, Haidian District, Beijing 100081, China. Tel.: +86-010-82106232. E-Mail: xubin@caas.cn (B. Xu).

Abstract

Accurate assessments of spatio-temporal patterns in net primary productivity and their links to climate are important to obtain a deeper understanding of the function, stability and sustainability of grassland ecosystems. We combined a satellite-derived NDVI time series dataset and field-based samples to investigate spatio-temporal patterns in aboveground net primary productivity (ANPP), and we examined the effect of growing-season air temperate (GST) and precipitation (GSP) on these patterns along a climate-related gradient in an eastern Eurasian grassland. Our results indicated that the ANPP fluctuated with no significant trend during 2001 to 2012. The spatial distribution of ANPP was heterogeneous and decreased from northeast to southwest. The interannual changes in ANPP were mainly controlled by year-to-year GSP; a strong correlation of interannual variability between ANPP and GSP was observed. Similarly, GSP strongly influenced spatial variations in ANPP, and the slopes of fitted linear functions of the GSP–ANPP relationship increased from arid temperate desert grassland to humid meadow grassland. An exponential function could be used to fit the GSP–ANPP relationship for the entire region. An improved moisture index that combines the effects of GST and GSP better explained the variations in ANPP compared with GSP alone. In comparisons with the previous studies, we found that the relationships between spatio-temporal variations in ANPP and climate factors were probably scale-dependent. We imply that the quantity and spatial range of analyzed samples contribute to these different results. Multi-scale studies are necessary to improve our knowledge of the response of grassland ANPP to climate change.

Keywords: temperate steppe; aboveground net primary productivity; remote sensing; spatio-temporal

patterns; growing-season air temperate; growing-season precipitation

1 Introduction

The net primary productivity of terrestrial vegetation is a key component of the global carbon (C) cycle, as its spatio-temporal patterns reflect the potential of vegetation to act as a carbon sink (Scurlock et al. 2002; Thurner et al. 2013). Among terrestrial ecosystems, Eurasian grasslands, which are located in arid and semi-arid regions, play an important role in regional carbon cycles because they have a widespread spatial distribution and a high proportion of biomass in roots (Ma et al. 2010). Furthermore, Eurasian grasslands provide a variety of ecological functions, including water and soil conservation, windbreak and sand fixation (Dai, 2016). Eurasian temperate grasslands are one of the most sensitive terrestrial ecosystems, where aboveground net primary productivity (ANPP) often shows dramatic spatio-temporal variations that are strongly influenced by rainfall (Knapp & Smith, 2001). Since grassland ANPP in this region is the basis for regional livestock production, it influences regional land-use patterns (Soussana et al. 2004). Investigating grassland ANPP and its climatic drivers is essential to understanding the potential role of grasslands in regional C cycles and the response of ANPP to climate change and for improving livestock management under future climate change scenarios (Reynolds et al. 2005; Fang et al. 2010).

Remote sensing is an efficient approach for monitoring vegetation dynamics at a large spatio-temporal scale because of its global coverage at relatively high temporal and spatial resolutions (Yang et al. 2009; Gao et al. 2012; Li et al. 2013). The normalized difference vegetation index (NDVI), which indicates the density and photosynthetic capacity of vegetation, is often combined with *in situ* measurements to estimate vegetation ANPP over broad areas (Piao et al. 2007; Xu et al. 2008; Ma et al. 2010; Zhao et al. 2012; Schweiger et al. 2015). At a national scale, for example, the interannual changes and spatial distribution of China's grassland biomass carbon stocks have been examined over the past two decades using Advanced Very High Resolution Radiometer (AVHRR) NDVI time-series data and ground-based observations (Piao et al. 2007; Ma et al. 2010). At a regional scale, the production of temperate grasslands in Xilingol has been estimated by combining Moderate Resolution Imaging Spectroradiometer (MODIS) NDVI data with ground-truth data collection at *in situ* sample sites (Kawamura et al. 2005; Jin et al. 2011). Although remote sensing images are the main source of data for large-scale spatial vegetation observations in these estimating processes, field-based samples are required for modeling NDVI–ANPP relationships and testing models. However, sufficient field sampling data are still relatively lacking for certain years due to the broad distribution of Eurasian temperate grasslands and their harsh conditions. Additionally, previous studies have evaluated ANPP using a single model, in which case the spatially varied relationships between ANPP and vegetation index may be ignored (Xu et al. 2008).

The impact of climate factors on the spatio-temporal patterns of ANPP is a key issue concerning the response of grassland ecosystems to climate change (Hsu et al. 2012). Precipitation is a principal climate factor that impacts temperate grassland ecosystem processes (Hu et al. 2010; Beier et al. 2012). Temporally, both field-based and remote sensing-based studies have suggested that year-to-year precipitation variation is a major factor driving interannual fluctuations of ANPP (Fang et al. 2001; Knapp & Smith 2001; Bai et al. 2004; Ma et al. 2010). As future climates are forecast to undergo greater precipitation variability, ecologists are increasingly interested in how future climate may influence precipitation variability and ANPP (Craine et al. 2012; Guo et al. 2012). However, the relationships between interannual ANPP variability and precipitation variability (usually expressed by coefficient of variation) are debated (Fang et al. 2001; Knapp & Smith 2001; Hu et al. 2007). At a spatial scale, linear relationships have been proposed between precipitation and ANPP of Eurasian temperate grasslands, but this view has been challenged by recent studies (Ma et al. 2008; Hu et al. 2010; Guo et al. 2012). For example, Guo et al. (2012) observed an exponential relationship between ANPP and precipitation for Inner Mongolian temperate grasslands. The increasing slope in the precipitation–ANPP relationship along a precipitation gradient can be explained by different precipitation-use efficiencies among various plant communities (Guo et al. 2012). Nevertheless, the quantity of samples and the utilized analytical methods limit our understanding of the nature of precipitation–productivity relationships (Hu et al. 2010; Siefert et al. 2012). Furthermore, temperature should be considered in any explanation of productivity variation. Climate warming may intensify water evaporation and thus induce drought, which contributes to the further loss of grassland productivity in arid and semi-arid regions (Huang & Anderegg 2012). This coupled temperature–precipitation effect on grassland productivity is poorly understood at a large spatio-temporal scale.

Inner Mongolia is located in the eastern Eurasian grassland, which contains the most important grassland resources in China (Fan et al. 2009). In this study, we used field-based samples, remote sensing time-series data and climatic data to investigate the spatio-temporal variations in ANPP and the effects of temperature and precipitation on these variations in the grasslands of Inner Mongolia. The main objectives of this research were to examine (1) the interannual changes and spatial distribution of grassland ANPP from 2001 to 2012 and (2) the relationships between spatio-temporal variations in ANPP and the climate factors. The latter objective mainly includes evaluating the relationship between the interannual variability of precipitation and ANPP and the coupled temperature–precipitation effect on the spatial variations in ANPP.

2 Materials and methods

2.1 Study area

The study region for this research was the Inner Mongolian grasslands in northern China, an important part of Eurasian temperate grasslands. This region is located throughout most of the Inner Mongolian Plateau and has a relatively flat topography and typical vegetation communities. Thus, due to the lack of additional variables that could complicate interpretations, this location is suitable for investigating ANPP variations in grasslands. The study region stretches across sub-humid, semi-arid and arid regions that are strongly affected by the Asian monsoon climate. Under the influence of Asian monsoons, annual precipitation levels exhibit a strong east–west gradient that decreases from more than 500 mm to less than 150 mm, mainly falling in the summer. The mean annual temperature of the study area ranges from −5 to 9°C. This wide climate gradient can allow us to systematically understand how spatial patterns of temperature and precipitation affect grassland ANPP. The grassland types are dominated by a temperate meadow steppe (dominant species of *Leymus chinensis*, *Stipa baicalensis*, *Stipa grandis*, etc.), a temperate steppe (dominant species of *L. chinensis*, *S. grandis*, *Agropyron cristatum*, etc.) and a temperate desert steppe (dominant species of *Agropyron desertorum*, *Stipa klemenzii*, *Cleistogenes songorica*, etc.) from the east to the west (Guo et al. 2012) (Fig. 1). Chernozem, chestnut and brown are the three zonal soils in this region (Genetic Soil Classification of China).

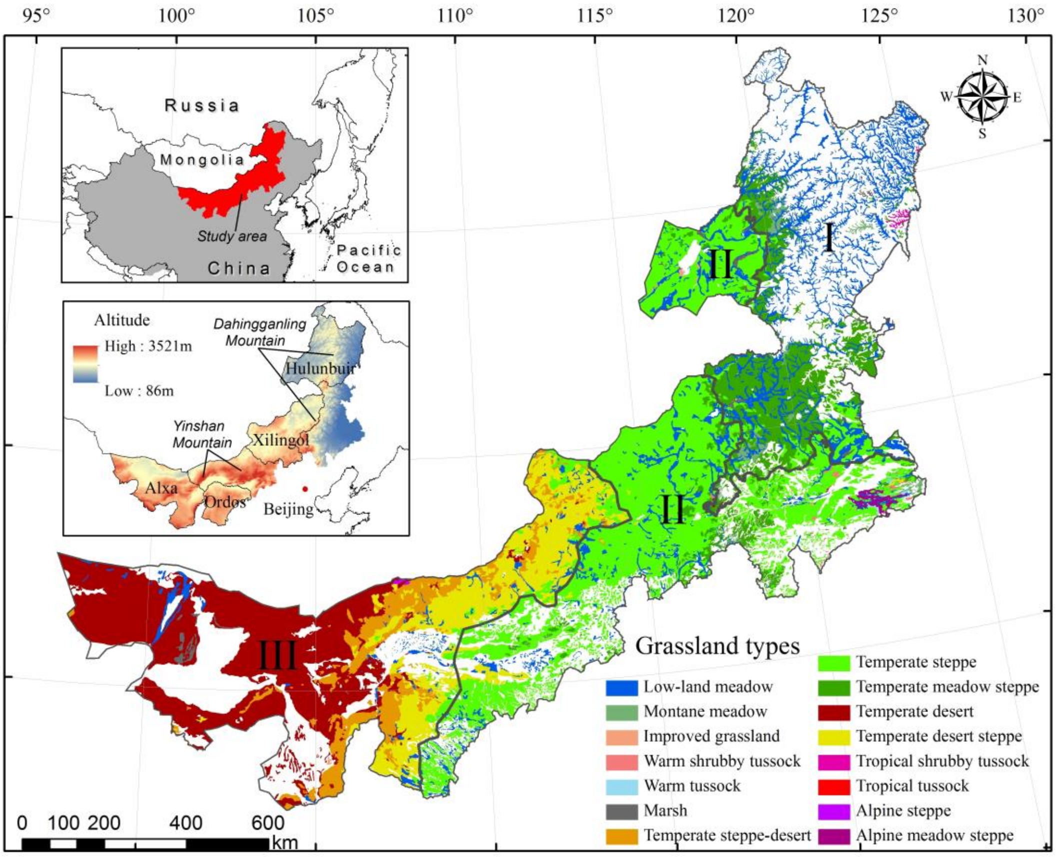

Fig. 1. Spatial distribution of grassland types in Inner Mongolia. Sub-region I is the eastern meadow grassland region; sub-region II is the middle temperate grassland region; and sub-region III is the western desert grassland and desert region (Department of Animal Husbandry Veterinary 1996).

2.2 *In situ* ANPP measurements

Field samples were obtained from eight consecutive large-scale field campaigns, mainly in July and August from 2005 to 2012. The sampling sites, each with an area of at least 1 km^2, were chosen to represent typical vegetation communities. For most sites, three plots (1 m×1 m) were selected, with the distance between plots greater than 250 m, and all aboveground plants in the plots, most of which were herbaceous, were harvested to measure their fresh grass yield (FGY). For shrubs, one plot (10 m×10 m) was sampled by measuring representative plants; green parts and bundled branches from the current year were cut to measure their FGY. A total of 3,634 field samples of FGY, which were represented by fresh weight were finally obtained to estimate *in situ* ANPP (Fig. 2).

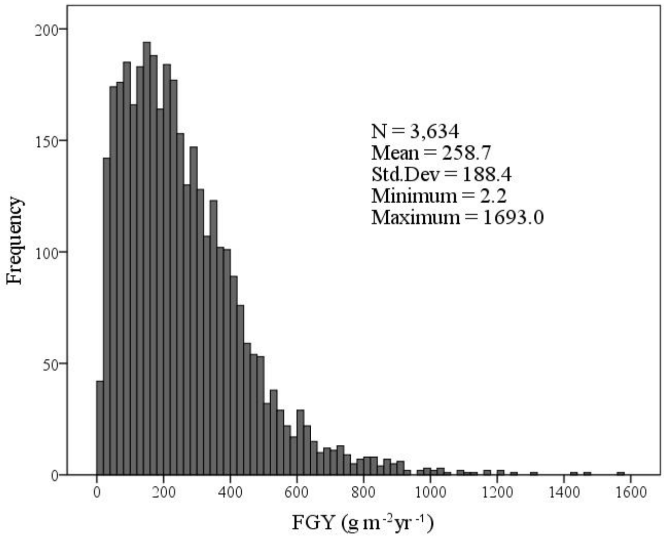

Fig. 2. Frequency distributions of the fresh grass yield (FGY).

2.3 Remote sensing data

The remote sensing data used in this study were taken from an NDVI time-series dataset at a spatial resolution of 250 m and based on 16-day composited products for the period from 2001 to 2012. These data were re-projected to Albers Equal Area projection with MODIS Reprojection Tool, and the monthly VI data were calculated using the Maximum Value Composition (MVC) method to minimize the effects of cloud cover, atmospheric perturbations, sunlight and viewing geometry (Goetz et al. 2006, Tang et al. 2010). Since the samples were collected during July and August, the NDVI of the peak season was then calculated using the average NDVI values for July and August. Then, we produced the spatial distribution of the NDVI data for the entire study area (Gao et al. 2013A). Because NDVI data in sparsely vegetated areas are largely influenced by the spectral characteristics of the soil, we only analyzed areas with a peak season NDVI >0.1 (Myneni et al. 2001; Fang et al. 2004).

2.4 Climate datasets and interpolation

Monthly mean air temperature and precipitation data from 2001 to 2012 were derived from 47 meteorological stations across Inner Mongolia and acquired from the National Meteorological Information Center (NMIC). To explore the effects of air temperature and precipitation on ANPP, we used the Anusplin 4.3 software package to interpolate and produce a continuous spatial distribution of temperature and precipitation data with a spatial resolution of 500 m (Hutchinson 2004; Guo et al. 2012; Luo et al. 2013; Zheng et al. 2013). An error analysis of the interpolation method in our study area presented a mean relative error (REE) of 10 to 30% for monthly precipitation and of <6% for the average monthly temperature during the growing season (Gao et al. 2013B). The error derived from the spatial interpolation of climate factors, especially precipitation, may be higher in areas far from meteorological stations. To reduce this uncertainty, we only extracted interpolation areas within 50 km of a meteorological station.

2.5 Remote sensing-based ANPP estimation

We adopted a conventional approach by establishing an empirical relationship between *in situ*-measured ANPP and MODIS NDVI data to estimate the ANPP of the entire region for the period of 2001 to 2012 (Xu et al. 2008; Guo et al. 2012; Irisarri et al. 2012). An ANPP model for a given region may fit the relationships between NDVI and ANPP values better than a model for a different region. We divided Inner Mongolia into three sub-regions (Fig. 1) and established an ANPP estimation model for each sub-region (Gao et al. 2013A).

We estimated the grassland ANPP using the following four steps. First, we calculated the mean NDVI value within a circular area of the plot (one of three plots in a sampling site; 250 m radius) (Xu et al. 2008); subsequently, we established a database for the actual site-specific FGY values versus the peak season NDVI values for each year. Second, we used this database to develop unitary linear, quadratic, power and exponential regression models and to evaluate the estimated model precision. As shown in Table 1, the optimal estimating functions for the eastern, middle and western sub-regions were the exponential, power and unitary linear functions, respectively. Third, we selected the best regression models to estimate the FGY for each pixel for the period from 2001 to 2012.

Table 1 Statistical models for FGY versus NDVI for the three sub-regions

Regions	models	R^2	F value	RMSE ($g\ m^{-2}\ yr^{-1}$)	REE (%)	Precision (%)
The eastern region	$Y=28.615e^{3.909x}$	0.65	1049.73	135.44	25.92	74.08
The middle region	$Y=850.2x^{1.6069}$	0.64	2630.07	83.27	27.40	72.60
The western region	Y=750.86x-51.47	0.57	1137.48	44.21	32.92	67.08

Note: 80% and 20% samples were used for modeling and evaluation, respectively. The RMSE and REE were calculated as $RMSE = \sqrt{\frac{\sum (Y_i - Y_i^{'})^2}{N}}$ and $REE = \sqrt{\frac{\sum \left[(Y_i - Y_i^{'}) / Y_i^{'}\right]^2}{N}}$, where Y_i is the actual ANPP (random reserved field samples), Y_i' is the estimated ANPP and N is the number of samples.

The field-based samples that were used to model the relationship between the FGY and NDVI values were expressed in terms of fresh weight. To obtain grassland ANPP, finally, the estimated wet yield was converted to air-dried weights according to conversion coefficients for different grassland types (Department of Animal Husbandry Veterinary 1996). The air-dried weights were then converted to dry weights, assuming a 15% water content (Fang et al. 1996). The estimated ANPP values were ultimately converted into units of carbon with a conversion factor of 0.45 (Fang et al. 1996).

2.6 Analysis of the relationships between ANPP and climatic factors

The growing season for temperate grasslands in Inner Mongolia is approximately from May to October (Piao et al. 2006; Cong et al. 2013), and the main period of carbon sequestration in grassland vegetation is from May to August (Xu et al. 2008). Thus, we calculated the main growing season (May to August) mean air temperature (GST) values and the main growing season total precipitation (GSP) levels. To examine the effects of climate factors on interannual changes in ANPP, we analyzed their relationships using an anomaly index (Ma et al. 2010). Furthermore, a coefficient of variation (CV) was introduced to express the magnitude of interannual ANPP and GSP variability.

Generally, interpolation accuracies of climate data decrease as the increasing distance between interpolated locations and climate stations. To promote reliability of analysis results, we extracted points within 50 km of climate stations by randomly selecting 100 points for each climate station and examined the effects of climate factors on the spatial variation of ANPP. For each point, we averaged the 12-year values of ANPP, GSP and GST to analyze their relationships. Moreover, we employed an improved moisture index K to examine the combined influence of the GSP and GST values (K=GSP/(accumulated GST×0.1) (Ren & Hu 1965; Hu et al. 2007). All statistical analyses were performed using the SPSS 17.0 software.

3 Results

3.1 Spatio-temporal patterns of grassland ANPP

The total amount of grassland ANPP averaged 20.9 TgC yr^{-1} over an area of 67.7×10^{4} km^{2} for the period from 2001 to 2012. Over these 12 years, ANPP in this study region fluctuated, showing no significant trend (R^2=0.03, P=0.57), with an annual ANPP CV of 10.5% being observed. None of the three sub-regions showed significant trends, but their interannual variabilities were different. The annual ANPP CV was 8.6% for the eastern sub-region, 12.4% for the middle sub-region and 22.5% for the western sub-region, showing an increasing trend from east to west.

The total ANPP over the study area was 30.8 gC m^{-2} yr^{-1} (Fig. 3). The ANPP was highly spatially heterogeneous. A high ANPP (>45 gC m^{-2} yr^{-1}) was observed in the Daxinganling Mountains in eastern Inner Mongolia; a medium ANPP (15 to 45 gC m^{-2} yr^{-1}) was observed in most parts of Xilingol and Hulunbuir in central Inner Mongolia; and a low ANPP (<15 gC m^{-2} yr^{-1}) was observed from western Xilingol to the Ordos Plateau in western Inner Mongolia. Overall, the grassland ANPP gradually decreased from the northeast to the southwest, which is consistent with the zonal grassland types, showing a climate-related spatial pattern.

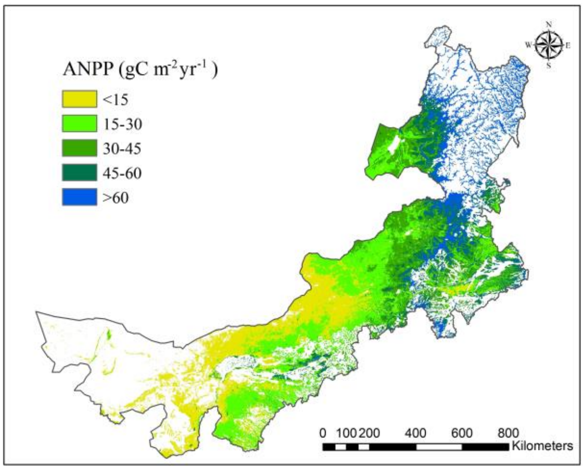

Fig. 3. Spatial distribution of the 12-year-averaged ANPP

3.2 Effects of climate variables on spatio-temporal patterns in grassland ANPP

The interannual ANPP dynamics were generally consistent with the year-to-year GSP variations over the entire study region (Fig. 4). For some years, however, negative correlations between GSP and ANPP were observed. These exceptional years were quantified by a definition that product of PAI (precipitation anomaly index) and ANPP-AI (anomaly index) was negative, and the absolute value of their differences was greater than 0.1 for a given year. There were three exceptions for the eastern sub-region (Fig. 4a), one exception for the middle sub-region (Fig. 4b), one exception for the western sub-region (Fig. 4c) and no exceptions for the study region as a whole (Fig. 4d). However, we did not find a strong relationship between the ANPP and GST values using the same method.

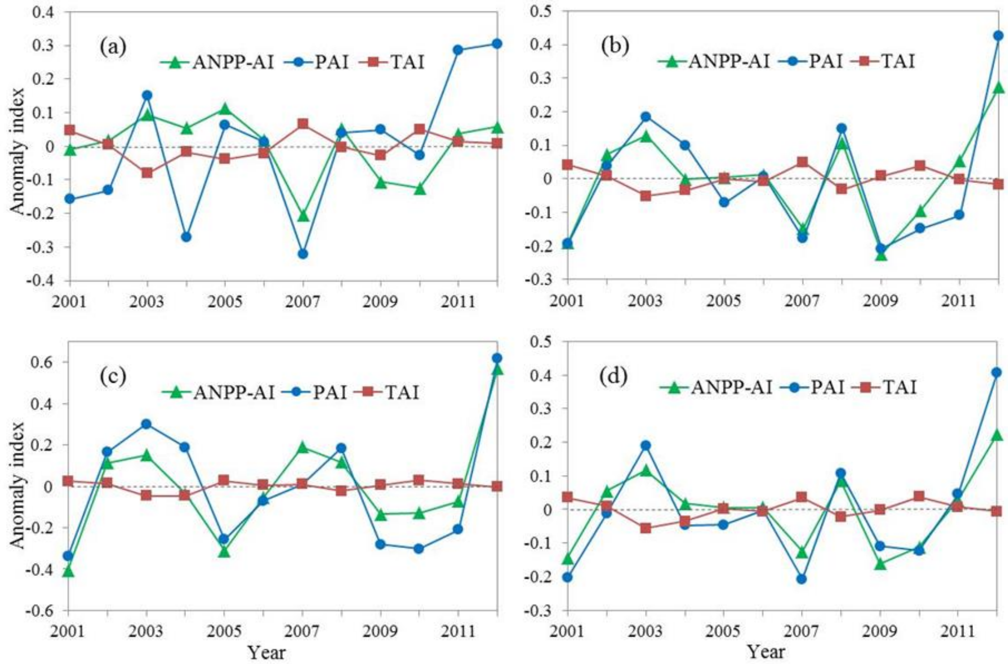

Fig. 4. Coupled interannual patterns between ANPP and climatic factors. (a) The eastern temperate meadow grassland region; (b) the middle temperate grassland region; (c) the western temperate desert grassland and desert region; (d) the Inner Mongolian grassland. ANPP-AI: ANPP anomaly index; TAI: temperature anomaly index; PAI: precipitation anomaly index. $ANPP\ \ AI = (ANPP_i - \overline{ANPP})/\overline{ANPP}$, where $ANPP_i$ is the ANPP of an individual year in Inner Mongolia, and $\overline{ANPP}$ is the mean ANPP from 2001 to 2012. PAI and TAI were calculated using the same method.

We introduced annual CVs to examine the effects of GSP on ANPP variability. As shown in Fig. 5a, there was a significant negative relationship between CV_{ANPP} and GSP, indicating that ANPP stability generally increased as the GSP gradient increased from west to east for the entire study region (R^2=0.43, P<0.001). The results also showed that grasslands in the humid region exhibited higher ANPP values and lower interannual variability compared with the arid region, which exhibited lower ANPP values and higher interannual variability. Furthermore, our statistical analysis showed a positive trend between CV_{ANPP} and CV_{GSP} (R^2=0.22, P<0.001; Fig. 5b), suggesting that the interannual variability of ANPP increased with GSP variability.

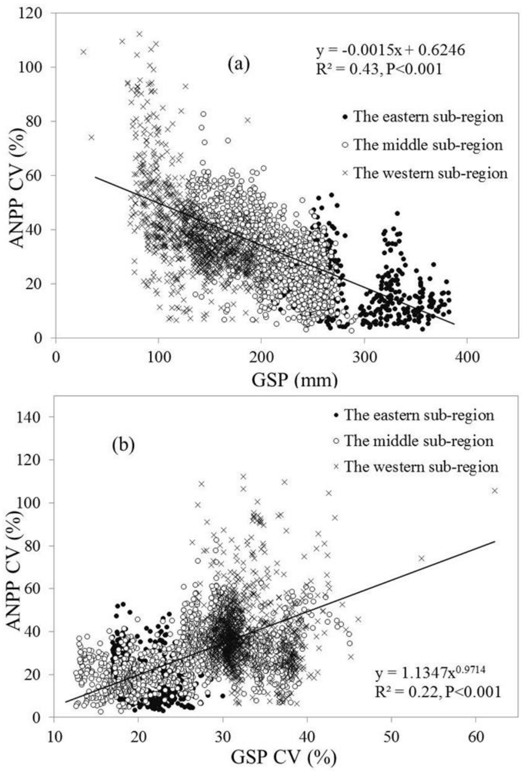

Fig. 5. (a) Interannual variability of ANPP (CV_{ANPP}) along a precipitation gradient in Inner Mongolian grasslands; (b) relationships between the interannual variability of annual growing season precipitation (CV_{GSP}) and that of ANPP (CV_{ANPP}) in Inner Mongolian grasslands.

We analyzed the relationships between the 12-year-averaged ANPP estimates and the interpolated climatic data and found that spatial variations in ANPP were partly controlled by GSP. As Fig. 6a illustrates, the ANPP of three sub-regions generally grouped at different precipitation intervals. For each sub-region, GSP could explain over 20% of the spatial variation of ANPP with the given linear function. The slope of the linear function for the eastern sub-region (0.2116) was steeper than the slopes for the middle sub-region (0.1497) and the western sub-region (0.0708). For the entire study region, the relationship between ANPP and GSP could be fit with an exponential function ($ANPP=2.7803e^{0.0098GSP}$, n=2907, $R^2=0.6818$, F=6224.53, P<0.001). Although a linear function and a power function could also be used to fit this relationship, the R^2 and *F* values were lower.

Conversely, differences in the GST of the three sub-regions were smaller (Fig. 6b). Higher temperatures were recorded in the western sub-region, whereas lower temperatures were recorded in the middle sub-region and the eastern sub-region. ANPP increased as GST decreased, but the correlation was weaker ($R^2=0.29$, P<0.001). Furthermore, ANPP showed a significant increase as the K value (moisture index) increased (Fig. 6c), which explained marginally more of the spatial variation in ANPP compared with GSP alone (70% vs. 68%).

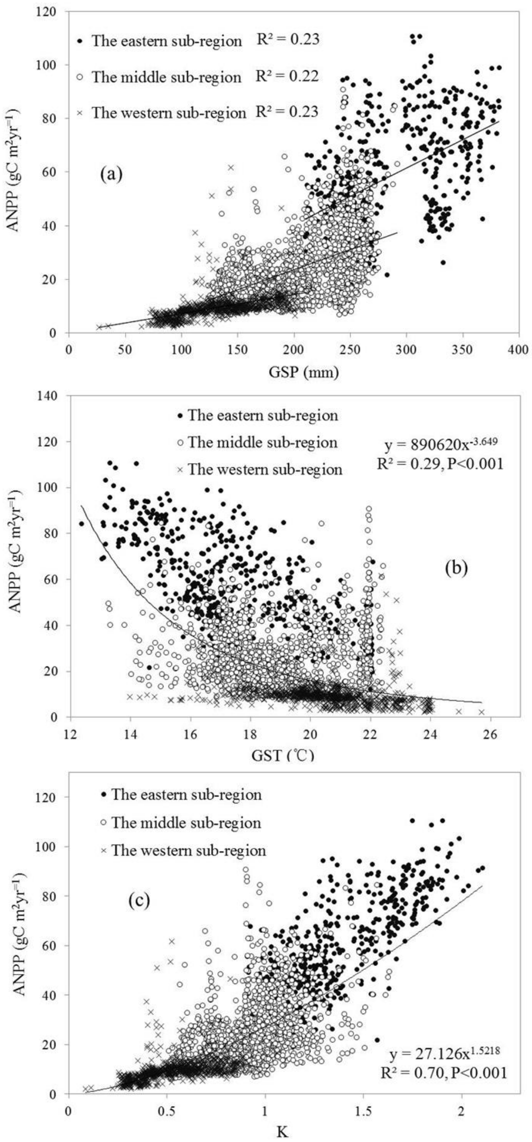

Fig. 6. Relationships between ANPP and climatic factors. (a) Growing season precipitation (GSP); (b) growing season temperature (GST); (c) moisture index (K). Each data point in the figure represents a 12-year average value for the period from 2001 to 2012.

4 Discussion

4.1 Effects of GSP on interannual changes in ANPP

Our findings indicate that the year-to-year variations in GSP were a predominant factor influencing the interannual changes in the ANPP of Inner Mongolian temperate grasslands. The middle sub-region and the western sub-region showed very similar interannual patterns of GSP–ANPP, whereas the trend that was observed in the eastern sub-region was weaker. These results suggest that interannual GSPs in the middle sub-region and the western sub-region dominate ANPP more strongly than that in the eastern sub-region. Some studies have suggested that an increase in temperature may promote vegetation productivity due to rising soil nitrogen availability and an extension of the growing season (Melillo et al. 2002; Piao et al. 2006; Piao et al. 2007). However, in the present study, we did not find that ANPP was strongly associated with GST, which did not support previous findings. Differences in the study regions might help to explain these contrasting results. Furthermore, our results indicated that the interannual variability of ANPP increased progressively as GSP decreased, implying that the stability of ANPP in temperate grassland ecosystems decreases with aridity. A significant positive trend was also revealed between the interannual ANPP and GSP variabilities. This finding does not support the results observed by Hu et al. (2007) and Knapp and Smith (2001). We inferred that this disagreement may be due to differences in the analyzed samples, including variable quantities and spatial ranges, which were caused by different observed scales and approaches. The main data used in the present study were satellite-derived NDVI time-series datasets and continuous spatial climate data; therefore, the analyzed samples were abundant in quantity and broad in their spatial distribution. Conversely, the data used in the studies of Knapp and Smith (2001) and Hu et al. (2007) were *in situ* samples from ground observation sites; thus the quantities and spatial extents of the analyzed data may be limited. These differences in methodology may have led to discrepancies in analytical results, such as the spatial trend of annual CV_{GSP}. For example, Hu et al. (2007) found that the interannual CV of precipitation did not show a well-defined trend across Inner Mongolia based on *in situ* data from 56 sites. Using 2,907 random points, nevertheless, we found that the interannual CV_{GSP} was negatively correlated with GSP

(R^2=0.35, P<0.001). It should be noted that the interannual CV_{ANPP} also showed a trend similar to that of GSP. In other words, both CV_{GSP} and CV_{ANPP} increase along the east–west precipitation gradient, thus leading to their similar positive trends.

4.2 Effects of GSP and GST on the spatial variation of ANPP

GSP also strongly affected the spatial variations in ANPP. Our findings suggest that ANPP increased exponentially as GSP increased from west to east in the Inner Mongolian temperate grasslands (R^2=0.68, P<0.001, Fig. 6a). We verified that the slope of the precipitation–ANPP relationship increased as the climate shifted from arid to humid, as reported by Guo et al. (2012). Linear relationships were also found between ANPP and precipitation in the temperate grasslands of Inner Mongolia (Bai et al. 2004; Fan et al. 2009). For example, Fan et al. (2009) reported a linear relationship between ANPP and precipitation on the basis of 48 sites. Differences in scale among the various studies may contribute to this disagreement in results. Hu et al. (2010) indicated that the slope of the precipitation–ANPP relationship may be variable if the analyzed samples are sufficient. This assumption was supported by the remote sensing-based study of Guo et al. (2012) and the results of the present study. In the present study, the randomly selected samples throughout Inner Mongolia grassland types that were derived from *in situ* ANPP measurements, remote sensing and climate data should constitute a powerful data source with which to examine the spatial relationship between GSP and ANPP.

Generally, the increasing slope of the precipitation–ANPP relationship along a precipitation gradient can be explained by differences in the precipitation-use efficiency of various grassland types (Huxman et al. 2004). In the humid eastern sub-region, vegetation communities have a relatively high leaf area index and plant biodiversity and can thus use water more efficiently (Bai et al. 2004; Hu et al. 2008). The different water use strategies of plant communities from different grassland types, including the conservative water use strategy of arid grassland plants and the open water use strategy of humid grassland plants, may also contribute to the increasing slope of the GSP–ANPP relationship (Webb et al. 1978; Paruelo et al. 1999; Guo et al. 2012). Therefore, in terms of the differences in precipitation-use efficiency for various grassland types, ANPP in humid grasslands seems to be more sensitive to altered GSP (Guo et al. 2012). Additionally, Inner Mongolia is characterized by a spatial pattern of warm-dry to cold-wet from west to east (Fig. 7). Thus, in the eastern sub-region, water for plants is relatively abundant due to not only high GSP values but also low rate of evaporation caused by the GST. Conversely, in the western sub-region, high GST values promote water evaporation and further intensify vegetation response to drought. This hydro-thermal spatial distribution should be considered when explaining the GSP–ANPP relationship.

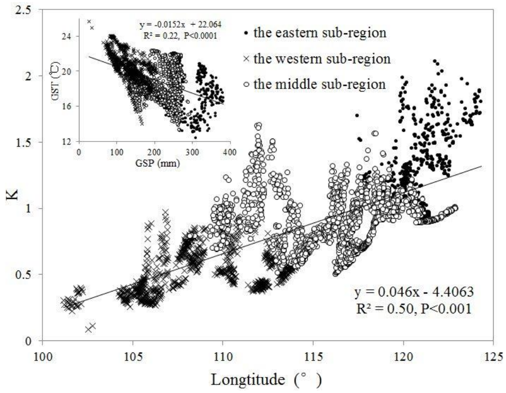

Fig. 7. Relationship between the moisture index (K) and longitude in Mongolian grasslands.

5 Conclusion

Field-based measurements and remote sensing and climate data together constituted a powerful data source that allowed us to investigate the spatio-temporal variations in vegetation ANPP and examine the effects of GST and GSP on these patterns in a Eurasian temperate grassland. The total amount of grassland ANPP was estimated to be 20.9 TgC yr^{-1}, although it generally fluctuated over time. The ANPP was 30.8 gC m^{-2} yr^{-1} over the entire area, and it gradually decreased from east to west. The interannual changes in ANPP were mainly driven by GSP, and a significant correlation was observed between the interannual variability of ANPP and GSP. Spatial variations in ANPP were also strongly affected by GSP, which increased exponentially as GSP increased from the west to the east along a GSP gradient. The rising slope of the fitted function may be explained by varying precipitation-use efficiencies of plants and GST–GSP spatial patterns. Our findings suggest that the relationships between spatio-temporal variations in ANPP and climatic factors, both temporally and spatially, are highly dependent upon the quantity and spatial range of the analyzed samples at different scales of observation. Therefore, multi-scale studies should be conducted to improve our knowledge of the effects of climate change on grassland ecosystems.

Acknowledgements

This study was funded by the National Natural Science Foundation of China (31372354, 41571105) and International Science & Technology Cooperation Program of China (2013DFR30760). We thank the Grassland Monitoring and Supervision Center of the Ministry of Agriculture for providing the ground-truth data. We also thank Dr. Yuanhe Yang for sharing *in situ* ANPP data, and we are grateful to Dr. Jiaojun Zhu for providing constructive suggestions on a draft of this manuscript.

References

Bai Y, Han X, Wu J, Chen Z, Li L (2004) Ecosystem stability and compensatory effects in the Inner Mongolia grassland. Nature 431: 181-184.

Beier C, Beierkuhnlein C, Wohlgemuth T, Penuelas J, Emmett B, Körner C, de Boeck H, Christensen JH, Leuzinger S, Janssens IA, Hansen K (2012) Precipitation manipulation experiments–challenges and recommendations for the future. Ecol Lett 15: 899-911.

Cong N, Wang T, Nan H, Ma Y, Wang X, Myneni R, Piao S (2013) Changes in satellite-derived spring vegetation green-up date and its linkage to climate in China from 1982 to 2010: a multi-method analysis. Global Change Biol 19: 881-891.

Craine JM, Nippert JB, Elmore AJ, Skibbe AM, Hutchinson SL, Brunsell NA (2012) Timing of climate variability and grassland productivity. P Natl Acad Sci USA 109: 3401-3405.

Department of Animal Husbandry and Veterinary Rangeland Resources of China (1996) Science and Technology Press, Beijing.

Dai E, Huang Y, Wu Z, Zhao D (2016) Analysis of spatio-temporal features of a carbon source/sink and its relationship to climatic factors in the Inner Mongolia grassland ecosystem. J Geogr Sci 26: 297-312.

Fan J, Wang K, Harrisc W, Zhong H, Hu Z, Han B, Zhang Y, Wang J (2009) Allocation of vegetation biomass across a climate-related gradient in the grasslands of Inner Mongolia. J Arid Environ 73: 521-528.

Fang J, Liu G, Xu S (1996) Carbon pools in terrestrial ecosystems in China, in emissions and their relevant processes of greenhouse gases in China. China Environment Science Press, Beijing.

Fang J, Piao S, Tang Z, Peng C, Ji W (2001) Interannual variability in net primary production and precipitation. Science 293: 1723 -1723.

Fang J, Piao S, He J, Ma W (2004) Increasing terrestrial vegetation activity in China, 1982–1999. Science in China Series C: Life Sciences 47: 229-240.

Fang J, Yang Y, Ma W, Mohammat A, Shen H (2010) Ecosystem carbon stocks and their changes in China’s grasslands. Science China Life Sciences 53: 757-765.

Gao T, Xu B, Yang X, Jin Y, Ma H, Li J, Yu D (2012) Review of researches on biomass carbon stock in grassland ecosystem of Qinghai-Tibetan Plateau. Progress in Geography 31: 1724-1731.

Gao T, Xu B, Yang X, Jin Y, Ma H, Li J, Yu H (2013A) Using MODIS time series data to estimate aboveground biomass and its spatio-temporal variation in Inner Mongolia's grassland between 2001 and 2011. Int J Remote Sens 34: 7796-7810.

Gao T, Yang X, Jin Y, Ma H, Li J, Yu H, Yu Q, Zheng X, Xu B (2013B) Spatio-temporal variation in vegetation biomass and its relationships with climate factors in the Xilingol grasslands, Northern China. Plos One 8: e83824.

Goetz SJ, Fiske GJ, Bunn AG (2006) Using satellite time-series data sets to analyze fire disturbance and forest recovery across Canada. Remote Sens Environ 101: 352-365.

Guo Q, Hu Z, Li S, Li X, Sun X, Yu G (2012) Spatial variations in aboveground net primary productivity along a climate gradient in Eurasian temperate grassland: effects of mean annual precipitation and its seasonal distribution. Global Change Biol 18: 3624-3631.

Hsu JS, Powell J, Adler PB (2012) Sensitivity of mean annual primary production to precipitation. Global Change Biol 18: 2246-2255.

Hu Z, Yu G, Fan J, Zhong H, Wang S, Li S (2010) Precipitation-use efficiency along a 4500-km grassland transect. 19: 842-851.

Hu Z, Fan J, Zhong H, Yu G (2007) Spatiotemporal dynamics of aboveground primary productivity along a precipitation gradient in Chinese temperate grassland. Science China Earth Sciences 50: 754-764.

Hu Z, Yu G, Fu Y, Sun X, Li Y, Shi P, Wang Y, Zheng Z (2008) Effects of vegetation control on ecosystem water use efficiency within and among four grassland ecosystems in China. Global Change Biol 14: 1609-1619.

Huang C, Anderegg WRL (2012) Large drought-induced aboveground live biomass losses in southern Rocky Mountain aspen forests. Global Change Biol 18: 1016-1027.

Hutchinson M (2004) Anusplin Version 4.3. Centre for Resource and Environmental Studies, Canberra, Australia.

Huxman TE, Smith MD, Fay PA, Knapp AK, Shaw MR, Loik ME, Smith SD, Tissue DT, Zak JC, Weltzin JF, Pockman WT, Sala OE, Haddad BM, Harte J, Koch GW, Schwinning S, Small EE, Williams DG (2004) Convergence across biomes to a common rain-use efficiency. Nature 429: 651-654.

Irisarri JGN, Oesterheld M, Paruelo JM, Texeira MA (2012) Patterns and controls of above-ground net primary production in meadows of Patagonia: A remote sensing approach. J Veg Sci 23: 114-126.

Jin Y, Xu B, Yang X, Li J, Wang D, Ma H (2011) Remote sensing dynamic estimation of grass production in Xilinguole, Inner Mongolia. Science China Life Sciences 41: 1185-1195.

Kawamura K, Akiyama T, Yokota H, Tsutsumi M, Yasuda T, Watanabe O, Wang G, Wang S (2005) Monitoring of forage conditions with MODIS imagery in the Xilingol steppe, Inner Mongolia. Int J Remote Sens 26: 1423-1436.

Knapp AK, Smith MD (2001) Variation among biomes in temporal dynamics of aboveground primary production. Science 291: 481-484.

Li Z, Tang B, Wu H, Ren H, Yan G, Wan Z, Trigo IF, Sobrino JA (2013) Satellite-derived land surface temperature: Current status and perspectives. Remote Sens Environ 131: 14-37.

Luo X, Chen X, Xu L, Myneni R, Zhu Z (2013) Assessing performance of NDVI and NDVI3 in monitoring leaf unfolding dates of the deciduous broadleaf forest in Northern China. Remote Sensing 5: 845-861.

Ma W, Yang Y, He J, Zeng H, Fang J (2008) Above- and below-ground biomass in relation to environmental factors in temperate grasslands, Inner Mongolia. Science China Life Sciences 38: 84-92.

Ma W, Fang J, Yang Y, Mohammat A (2010) Biomass carbon stocks and their changes in northern China's grasslands during 1982–2006. Science China: Life Sciences 53: 841-850.

Melillo JM, Steudler PA, Aber JD, Newkirk K, Lux H, Bowles FP, Catricala C, Magill A, Ahrens T, Morrisseau S (2002) Soil warming and carbon-cycle feedbacks to the climate system. Science 298: 2173-2176.

Myneni RB, Dong J, Tucker CJ, Kaufmann RK, Kauppi PE, Liski J, Zhou L, Alexeyev V, Hughes MK (2001) A large carbon sink in the woody biomass of Northern forests. P Natl Acad Sci USA 98: 14784 -14789.

Paruelo JM, Lauenroth WK, Burke IC, Sala OE (1999) Grassland precipitation-use efficiency varies across a resource gradient. Ecosystems 2: 64-68.

Piao S, Fang J, Zhou L, Tan K, Tao S (2007) Changes in biomass carbon stocks in China’s grasslands between 1982 and 1999. Global Biogeochem Cy 21: GB2002 DOI: 10.1029/2005GB002634.

Piao S, Mohammat A, Fang J, Cai Q, Feng J (2006) NDVI-based increase in growth of temperate grasslands and its responses to climate changes in China. Global Environ Chang 16: 340-348.

Ren J, Hu Z (1965) Bio-climate index for the first class of Chinese. Journal of Gansu Agricultural University 2: 33-40.

Reynolds S, Batello C, Baas S, Mack S (eds.) (2005) Grassland and forage to improve livelioods and reduce poverty. In: Grassland: A Global Resource. Wageningen Academic Publisher, Wageningen, The Netherlands.

Scurlock JMO, Johnson K, Olson RJ (2002) Estimating net primary productivity from grassland biomass dynamics measurements. Global Change Biol 8: 736-753.

Schweiger AK, Risch AC, Damm A, Kneubühler M, Haller R, Schaepman ME, Schütz M (2015) Using imaging spectroscopy to predict above-ground plant biomass in alpine grasslands grazed by large ungulates. J Veg Sci 26: 175-190.

Siefert A, Ravenscroft C, Althoff D, Alvarez-Yépiz JC, Carter BE, Glennon KL, Heberling JM, Jo IS, Pontes A, Sauer A, Willis A, Fridley JD (2012) Scale dependence of vegetation-environment relationships: a meta-analysis of multivariate data. J Veg Sci 23: 942-951.

Soussana JF, Loiseau P, Vuichard N, Ceschia E, Balesdent J, Chevallier T, Arrouays D (2004) Carbon cycling and sequestration opportunities in temperate grasslands. Soil Use Manage 20: 219-230.

Tang R, Li Z, Tang B (2010) An application of the Ts–VI triangle method with enhanced edges determination for evapotranspiration estimation from MODIS data in arid and semi-arid regions: Implementation and validation. Remote Sens Environ 114: 540-551.

Thurner M, Beer C, Santoro M, Carvalhais N, Wutzler T, Schepaschenko D, Shvidenko A, Kompter E, Ahrens B, Levick SR, Schmullius C (2013) Carbon stock and density of northern boreal and temperate forests. Global Ecol Biogeogr 23: 297-310.

Webb W, Szarek S, Lauenroth W, Kinerson R, Smith M (1978) Primary productivity and water use in native forest, grassland, and desert ecosystems. Ecology 59: 1239-1247.

Xu B, Yang X, Tao W, Qin Z, Liu H, Miao J, Bi Y (2008) MODIS-based remote sensing monitoring of grass production in China. Int J Remote Sens 29: 5313-5327.

Yang Y, Fang J, Pan Y, Ji C (2009) Aboveground biomass in Tibetan grasslands. J Arid Environ 73: 91-95.

Yang Y, Fang J, Ma W, Guo D, Mohammat A (2010) Large-scale pattern of biomass partitioning across China's grasslands. Global Ecol Biogeogr 19: 268-277.

Zhao X, Zhou D, Fang J (2012) Satellite-based studies on large-scale vegetation changes in China. J Integr Plant Biol 54: 713-728.

Zheng X, Zhu J, Yan Q (2013) Monthly air temperatures over northern china estimated by integrating MODIS data with GIS techniques. J Appl Meteorol Clim 52: 1987-2001.